Post-thaw *N*-acetylcysteine treatment promotes the recovery of cryopreserved spermatogonial stem cells

Eun-Ji Paeng[1,†], Sang-Eun Jung[1,2,†], Hyo Jin Gu[1], Sung-Hwan Moon[1], Seung Hee Shin[1], Buom-Yong Ryu[1,*]

[1]Department of Animal Science and Technology, Chung-Ang University, Anseong, Gyeonggi-Do 17546, Republic of Korea

[2]Current address: Laboratory of Cell & Gene Therapy, College of Pharmacy, Seoul National University, Seoul 08826, Republic of Korea

[†]These authors contributed equally to this work.

*Corresponding author: Buom-Yong Ryu, Ph.D., Department of Animal Science and Technology, Chung-Ang University, Anseong, Gyeonggi-Do 17546, Republic of Korea; E-mail: byryu@cau.ac.kr; Tel: +82-31-670-4687; Fax: +82-31-676-0062; ORCID: 0000-0002-8349-7299

ABSTRACT

Spermatogonial stem cells (SSCs) are essential for male fertility but are highly vulnerable to oxidative damage during cryopreservation. This study investigated whether short-term antioxidant treatment during early post-thaw recovery improves SSC viability and function. Murine germ cells enriched for SSCs were cryopreserved and treated with *N*-acetylcysteine for 12 h immediately after thawing, followed by 6.5 days of culture without supplementation. Treatment with 0.4 mM *N*-acetylcysteine significantly enhanced post-thaw proliferation (128.2 ± 6.9%, $p < 0.05$) compared with vehicle control. Comparable to α-tocopherol, *N*-acetylcysteine markedly reduced intracellular reactive oxygen species concentrations to near-baseline levels and attenuated the activation of apoptosis-related proteins, including FAS, caspase-8, cytochrome c, and caspase-3/7. Importantly, *N*-acetylcysteine treatment preserved undifferentiated spermatogonia marker expression and significantly increased functional recovery in vivo, as demonstrated by a higher total number of SSC-derived colonies following transplantation (889.7 ± 686.4 vs. 1903.5 ± 1616.9 colonies, $p < 0.05$). Collectively, these findings identify early post-thaw redox modulation as a critical determinant of SSC recovery and establish *N*-acetylcysteine treatment as a practical adjunct to cryopreservation protocols for fertility preservation in animal reproduction.

Keywords: Spermatogonial stem cells; Cryopreservation; Post-thaw recovery; Oxidative stress; *N*-acetylcysteine; Fertility preservation

1. Introduction

Spermatogonial stem cells (SSCs) are undifferentiated male germline stem cells that reside in the testicular niche and are essential for lifelong spermatogenesis [1]. Through asymmetric division, SSCs maintain the stem cell pool while generating differentiated germ cells that eventually develop into mature spermatozoa [2-6]. Their preservation is critical for sustaining male fertility and enabling the transmission of genetic information across generations. Given the increasing impact of environmental and societal factors on male fertility, preserving SSCs as a strategy for maintaining long-term fertility has become increasingly important [7].

Cryopreservation plays a central role in SSC-based fertility preservation, particularly in prepubertal males, a concern shared across clinical and animal reproductive contexts. Cryopreservation enables SSC long-term storage and offers the potential for subsequent autologous transplantation [8-10]. Despite its promise, cryopreservation often results in considerable cellular damage owing to extreme temperature shifts, reducing post-thaw viability [11]. The optimization of cryopreservation protocols is essential for improving SSC survival and enhancing their therapeutic applicability [12, 13]. In animal reproduction, SSC cryopreservation is likewise relevant for fertility preservation, genetic resource conservation, and assisted reproduction in livestock and experimental models. To date, however, most efforts to improve SSC cryopreservation have focused primarily on freezing conditions and cryoprotectant formulations, whereas the

immediate post-thaw recovery phase has received comparatively less attention as a potential intervention window [14, 15].

A major challenge in cryopreservation is the accumulation of reactive oxygen species (ROS) during freezing and thawing processes [16]. While low-level ROS production facilitates normal cell signaling, excessive ROS levels lead to oxidative stress, causing damage to cellular membranes, DNA, and mitochondria [17]. This activates apoptotic pathways, particularly the intrinsic pathway, via cytochrome c release and the activation of caspase cascades. Excessive apoptosis, especially within the first 12–24 h after thawing, has been identified as a key factor limiting the recovery and function of cryopreserved SSCs [11, 18]. These observations suggest that the early post-thaw period is not merely a passive recovery stage, but rather a biologically active phase during which cryoinjury continues to develop and may therefore be therapeutically targetable [11, 19].

The prevention of early post-thaw apoptosis is a recognized mechanism by which cryoprotectants improve cell recovery [20]. While endogenous antioxidant enzymes, such as superoxide dismutase and catalase, help neutralize ROS, accumulating evidence suggests that exogenous antioxidants can further enhance cytoprotection during the early recovery phase**.** Accordingly, supplementation with antioxidants immediately after thawing has been shown beneficial effects in various cell types, including sperm, embryo, and stem cells, by reducing ROS-induced apoptosis and improving post-thaw viability [16, 21,

22]. In line with these observations, our previous study demonstrated that α-tocopherol (α-TCP) improves post-thaw recovery of SSCs, highlighting oxidative stress as a major contributor to early cryoinjury [22]. Together, these findings support the concept that transient antioxidant treatment during early post-thaw recovery may represent a practical strategy to improve SSC survival without requiring modification of established freezing protocols [22]. Building on this established foundation, the present study focuses on identifying an antioxidant better suited for practical, short-term post-thaw intervention.

Based on these findings, we hypothesized that post-thaw antioxidant treatment of murine SSCs would attenuate ROS-induced apoptosis and promote functional recovery, thereby providing an effective strategy for improving male fertility preservation outcomes. Specifically, we investigated whether short-term N-acetylcysteine (NAC) treatment during the early post-thaw period could reduce oxidative stress, preserve the phenotype of germ cells enriched for SSCs, and improve functional recovery as assessed by in vivo transplantation. Such improvements in post-thaw SSC recovery might contribute to assisted reproduction, fertility preservation, and genetic resource conservation during animal reproduction.

2. Materials and methods

2.1. Ethics statement

All experimental procedures in animals were conducted in accordance with the *Guide for the Care and Use of Laboratory Animals* (National Institutes of Health) and were approved by the Institutional Animal Care and Use Committee of Chung-Ang University, Seoul, South Korea (IACUC Number: 202000104).

2.2. Animals

To isolate germ cells enriched for SSCs, C57BL/6-TG-EGFP (designated as C57-EGFP; Jackson Laboratory, Bar Harbor, ME, USA) and C57BL/6 (designated as C57; Samtako Bio Korea, Osan, Gyeonggi-do, South Korea) mice were used as donors and recipients, respectively. Donor-derived germ cells from C57-EGFP mice were identified based on enhanced green fluorescent protein (EGFP) expression assessed by fluorescence microscopy. All animals were maintained in the animal facility at the Chung-Ang University (License No. LML-08-466) under controlled environmental conditions (23 ± 1°C, 55 ± 10% relative humidity) with a 12 h light/dark cycle. These donor animals were subsequently used for germ cells enriched for SSCs isolation and in vitro expansion as described below.

2.3. Isolation and in vitro culture of germ cells enriched for SSCs

Unless otherwise specified, all reagents were obtained from Sigma-Aldrich (St. Louis, MO, USA). Testes were collected from 6–8-day-old C57-EGFP pups to isolate $EGFP^+$ germ cells enriched in SSCs. After removing the tunica albuginea, the seminiferous tubules were rinsed with Dulbecco's phosphate-buffered saline (DPBS; Gibco, Grand Island, NY, USA; 14200-075). Tubules were then digested in a 2:1 solution of 0.25% trypsin-EDTA (1×; Gibco; 25200-072) and 7 mg/mL DNase I (Roche, Basel, Switzerland; 10104159001) at 37°C for 5 min to obtain a single-cell suspension. The enzymatic reaction was neutralized by adding fetal bovine serum (FBS; GW Vitek, Seoul, South Korea; US-FBS-500) at 10% of the initial trypsin volume. The cell suspension was filtered through a 40 μm nylon mesh (SPL Life Sciences, Pocheon, Gyeonggi-do, South Korea) and centrifuged at 600 × *g* for 6 min at 4°C. The cell pellet was resuspended in Dulbecco's modified Eagle's medium (DMEM; Biowest, Nuaillé, France; L0103-500) supplemented with 10% FBS, 2 mM L-glutamine (Gibco, Waltham, MA, USA; 25030), 0.1 mM β-mercaptoethanol, 100 U/mL penicillin and streptomycin (Gibco, Waltham; 15140122), and 40 mM sodium bicarbonate. The cell number was determined using the trypan blue exclusion assay. To eliminate cellular debris, the suspension was carefully layered over 30% Percoll and centrifuged at 600 × *g* for 10 min at 4°C. Cells were incubated with anti-Thy-1 antibody microbeads (1:10 dilution; Miltenyi Biotech, Auburn, CA, USA; 130-049-101) in DPBS containing 1% FBS for 20 min at 4°C with gentle agitation.

Thy-1$^+$ cells were isolated using magnetic-activated cell sorting and seeded at a density of 0.2×10^6 cells per well in 24-well culture plates.

The cells were cultured on mitomycin C-treated STO feeder cells in a defined mouse serum-free medium (mSFM) supplemented with three growth factors: 10 ng/mL glial cell line-derived neurotropic factor (GDNF; R&D Systems, Minneapolis, MN, USA; 212-GD-50), 75 ng/mL GDNF family receptor alpha 1 (GFRα1; R&D Systems; 560-GR-100), and 1 ng/mL basic fibroblast growth factor (bFGF/FGF2; BD Biosciences, San Jose, CA; 354060), as previously described [23]. STO feeder cells (CRL-1503, ATCC, Manassas, VA, USA) were pre-seeded at a density of 0.1×10^6 cells per well in 24-well plates 1–2 days prior to SSC seeding. The culture medium was replaced every 2–3 days, and the cultured germ cells were passaged every week by trypsinization.

2.4. Cryopreservation

Germ cells enriched for SSCs (1.0×10^5) were suspended in 500 μL of 400 mM trehalose and then the suspension was immediately diluted in a dropwise manner with the same volume of cryoprotectant containing DPBS with 20% dimethyl sulfoxide (DMSO) and 20% FBS (v/v). The final mixture contained 200 mM trehalose, 10% DMSO, and 10% FBS in DPBS [24]. To allow trehalose permeation, cell suspensions were incubated at room temperature for 20 min prior to aliquoting into 1.8 mL cryovials (SPL Life Sciences). Cryovials were placed in

a Mr. Frosty freezing container (Nalgene, Rochester, NY, USA) filled with isopropyl alcohol and stored at −80°C overnight to achieve a controlled freezing rate of approximately −1°C/min.

Thawing was performed after at least one month of storage. The frozen germ cells enriched for SSCs were thawed in a water bath at 37°C for 2.5 min. Each cell suspension was diluted 1:10 in a the dropwise manner using minimum essential medium alpha (MEMα; Gibco, Waltham; 12000) containing 10% FBS. Cells were centrifuged at 600 × *g* for 6 min at 4°C, and viability was assessed using trypan blue exclusion. The cell survival rate (%) was calculated using the following equation:

Survival rate = (Number of viable cells / Total number of cells) × 100

2.5. Post-thaw culture of germ cells enriched for SSCs with antioxidants

Following thawing, germ cells enriched for SSCs were seeded onto STO feeder layers and cultured in mSFM supplemented with growth factors (GDNF, GFRα1, and bFGF) and antioxidants. The control group received no antioxidant treatment, whereas 0.4 mM α-TCP (Sigma-Aldrich; T3251) was used as a positive control [22]. Stock solutions of *N*-acetylcysteine (NAC; Sigma-Aldrich; A7250), sodium selenite (Sigma-Aldrich; 214485), and parthenolide (EMD Millipore, Billerica, MA, USA; 512732) were prepared in DPBS (for NAC and selenite) or DMSO (for parthenolide) and diluted 1:1000 in mSFM. The final concentrations

were determined based on previous studies [25]. Cells were incubated with antioxidant-containing media at 37°C and 5% CO_2 for 12 h, a period during which cryodamage is most acute [18, 22]. After the 12 h treatment period, the culture medium was carefully replaced by slow aspiration, leaving a small residual volume (~5%) to minimize cell detachment. Cells were then cultured for an additional 6.5-day in antioxidant-free mSFM containing growth factors. After culturing, cells were dissociated using 0.25% trypsin, centrifuged at 600 × *g* for 6 min at 4°C, and resuspended in mSFM. Proliferation was assessed by cell counting and calculated using the following equation:

Proliferation rate (%) = (Number of harvested cells / Number of seeded cells) × 100

Relative proliferation rate (%) = (Proliferation rate of treatment group / Proliferation rate of control group) × 100

2.6. ROS detection using DCFDA

To assess cryopreservation-induced oxidative stress, intracellular ROS levels were measured using 2′,7′-dichlorofluorescein diacetate (DCFDA; Millipore, 287810). Cells treated with or without antioxidants were incubated for 12 h at 37°C in mSFM, followed by the addition of 10 μM DCFDA. After 45 min of incubation, 4 μg/mL Hoechst 33342 (Sigma-Aldrich; B2261) was added and incubated for 10 min to stain nuclei. The staining solution was then replaced with

cold DPBS, and fluorescence images were captured using a TS-1000 fluorescence microscope equipped with NIS Elements imaging software (Nikon, Tokyo, Japan). ROS fluorescence intensity was quantified using the ImageJ software (version 1.8.0; National Institutes of Health, Bethesda, MD, USA). For each treatment group, five randomly selected representative fields were analyzed.

2.7. Western blot analysis of apoptosis-related markers

To evaluate apoptosis after cryopreservation, western blotting was performed to assess the expression of apoptosis-related proteins. Germ cells enriched for SSCs were harvested 12 h after antioxidant treatment and lysed in Totex lysis buffer (20 mM HEPES [pH 7.9], 150 mM NaCl, 20% glycerol, 1% NP-40, 1 mM $MgCl_2$, and 0.5 mM EDTA) containing a protease inhibitor cocktail [25]. The protein concentration was determined using the Bradford assay (Bio-Rad, Hercules, CA, USA; 5000006). Equal amounts of protein (10–30 μg) were separated by 15% SDS-PAGE and transferred to methanol-activated polyvinylidene difluoride membranes (Millipore; IPVH00010). Membranes were blocked with 5% skim milk in PBS-T (DPBS, containing 0.1% Tween 20) for 30 min at room temperature and incubated overnight at 4°C with primary antibodies (1:1000 dilution) targeting apoptosis-related proteins from extrinsic (FAS and caspase-8) and intrinsic (BCL-2, BAX, cytochrome c, and caspase-9) pathways, as well as execution-phase markers (caspase-3 and caspase-7) and the loading

control α-tubulin. After washing, the membranes were incubated with horseradish peroxidase-conjugated secondary antibodies (1:5000 dilution) for 1 h at room temperature. Bands were visualized using Clarity™ Western ECL Substrate (Bio-Rad; 1705061) and imaged using a Touch Imager (e-BLOT Life Science, Shanghai, China). Band intensities were quantified using ImageJ software and normalized to the loading control, α-tubulin. A detailed list of all antibodies used for western blot analysis is provided in Table S1.

2.8. Immunocytochemistry

To examine the effects of the antioxidants on germ cells enriched for SSCs characteristics during cryopreservation and thawing, immunocytochemistry was performed to assess the expression of undifferentiated spermatogonia-specific proteins. Freeze–thawed germ cells enriched for SSCs were cultured in vitro for one week, dissociated, and fixed with 4% paraformaldehyde (Biosesang, Seongnam, Gyeonggi-do, South Korea) for 30 min at room temperature in the dark with gentle shaking. Fixed cells were centrifuged at 600 × *g* for 6 min at 4°C, and the pellet was resuspended in 100 mM sucrose (Sigma-Aldrich; S1888). Approximately 0.02×10^6 cells were seeded onto PTFE-printed slides (Thermo Fisher Scientific, Waltham, MA, USA; 63425-05) and air-dried for 20–30 min at room temperature. To facilitate antibody penetration, cells were permeabilized using DPBS containing 0.1% Triton X-100 (v/v) for 15 min at room temperature.

Nonspecific binding sites were blocked with 5% bovine serum albumin (BSA) in a humidified chamber for 30 min. Cells were then incubated overnight at 4°C with primary antibodies diluted 1:100. After washing with DPBS, secondary antibodies (1:200 dilution) were added under light-protected conditions, and the samples were incubated for 1 h at room temperature. The antibodies used for immunocytochemistry are listed in Table S2. Nuclear staining was performed using VectaShield® mounting medium containing 4,6-diamidino-2-phenylindole (DAPI; LSBio, Seattle, WA, USA). Marker expression was observed using fluorescence microscopy. To ensure nonredundant quantification, five randomly selected representative fields were analyzed for each condition.

2.9. In vivo transplantation

To eliminate endogenous germ cells, male recipient C57 mice (6 weeks old) were treated with 45 mg/kg busulfan before donor cell transplantation. Germ cells enriched for SSCs at low passage (8–11 passages) were used. Following cryopreservation, thawing, and culture, cells were adjusted to a final concentration of 1.0×10^6 cells/mL. Recipient mice were anesthetized with ketamine (75 mg/kg) and medetomidine (0.5 mg/kg), and donor cells were transplanted into the seminiferous tubules via the efferent ducts, as previously described [26, 27]. Two months after transplantation, the recipient testes were collected, decapsulated, and analyzed for colony formation. Colonies of donor-

derived $EGFP^+$ SSCs exceeding 1 mm in length were counted under a fluorescence microscope [28]. To assess SSCs functionality after cryopreservation, the number of colonies formed per 1.0×10^5 transplanted cells was calculated using the following equation:

Colonies per 10^5 transplanted cells = (Number of colonies × 10^5) / Number of transplanted cells

To evaluate the protective effect of cryopreservation with 0.4 mM NAC, the total colony yield was also calculated relative to the total number of cultured germ cells enriched for SSCs after cryopreservation:

Colonies per total number of cultured SSCs after cryopreservation = (Number of colonies × Total number of cultured cells) / Number of transplanted cells

2.10. Hematoxylin and eosin staining

Seminiferous tubules were fixed in 4% paraformaldehyde (Biosesang; P2031), paraffin-embedded, and sectioned at a thickness of 4 μm. The paraffin sections were deparaffinized in xylene and rehydrated using a graded ethanol series. Sections were stained with Harris hematoxylin for 7 min, rinsed with distilled water, and counterstained with Eosin Y (Sigma-Aldrich; E6003) for 3 min. Sections were dehydrated using graded ethanol, cleared in xylene, and mounted.

2.11. Immunohistochemistry

H&E and immunohistochemistry tissue sections were prepared from sequential, consecutive sections of the same paraffin-embedded testis samples. Images represent adjacent sections from the same seminiferous tubule. Immunohistochemistry was performed according to a previously published protocol [29], with minor modifications. Paraffin-embedded sections were deparaffinized in xylene (DUKSAN, Daejeon, South Korea; 2942) and rehydrated in graded ethanol (100%, 80%, 70%, and 50%). Antigen retrieval was performed in citrate buffer (pH 6.0) in a water bath at 95°C for 30 min. Sections were incubated in DPBS containing 1% SDS to enhance antigen accessibility, followed by blocking with 5% BSA in 0.1% Triton X-100 for 1 h at room temperature in a humidified chamber.

Sections were incubated overnight at 4°C with a rabbit polyclonal anti-GFP antibody (Abcam, Cambridge, UK; ab290) diluted 1:50 in 5% BSA. After washing with DPBS, the sections were incubated with Alexa Fluor 488-conjugated donkey anti-rabbit secondary antibody (Invitrogen, Carlsbad, CA, USA; A21206) diluted 1:200 in 5% BSA for 2 h at room temperature. Following DPBS washes, the sections were stained with Alexa Fluor 647-conjugated peanut agglutinin (PNA) lectin (Invitrogen; L32460) diluted 1:100. Sections were mounted using VECTASHIELD® mounting medium containing DAPI (LifeSpan BioSciences, Seattle, WA, USA; LS-J1032).

2.12. Statistical analysis

Statistical analyses were performed using the GraphPad Prism software (version 8.0.1; GraphPad, La Jolla, CA, USA). One-way analysis of variance (ANOVA) was used for group comparisons, followed by Tukey's post-hoc test for multiple comparisons. For comparison between two groups in the in vivo transplantation experiment, the unpaired two-tailed Student's *t*-test was used. All data are presented as the mean ± SEM, and the significance level was set at $p < 0.05$.

3. Results

3.1. NAC 0.4 mM restores the proliferative capacity of germ cells enriched for SSCs following cryoinjury

To examine the effects of NAC during early post-thaw recovery, $EGFP^+$ germ cells enriched for SSCs were cryostored in liquid nitrogen for more than one month, thawed, and exposed to NAC for the first 12 h after thawing followed by 6.5 days of standard culture (Fig. 1A). Post-thaw proliferation, ROS accumulation, apoptosis signaling, maintenance of SSC markers, and functional recovery after transplantation were examined.

Three antioxidants (NAC, sodium selenite, and parthenolide) were initially screened in the concentration range 0.01–1 mM. Sodium selenite (0.01 μM, 117.0 ± 5.9%; 0.1 μM, 117.8 ± 5.2%; 1 μM, 62.0 ± 5.6%) did not differ

significantly from the vehicle (100.0 ± 0.2%). In contrast, NAC 0.1 mM (129.9 ± 7.0%) and parthenolide 2 μM (121.9 ± 5.7%) increased proliferation relative to the vehicle (100.0 ± 0.2%), and NAC was selected for further experiments (Fig. S1). α-TCP 0.4 mM was used as a positive control, as described in our previous study [22]. Subsequent titration identified NAC 0.4 mM (128.2 ± 6.9%) as the optimal concentration, resulting in proliferation rates comparable to those after administration of α-TCP 0.4 mM (129.2 ± 4%; Fig. 1B–D). Microscopy confirmed larger and more compact $EGFP^+$ colonies in the NAC-treated group (Fig. 1C).

3.2. NAC effectively attenuates freeze–thaw-induced ROS accumulation

Intracellular ROS levels were measured using DCFDA after thawing. Vehicle-treated germ cells enriched for SSCs exhibited a marked increase in ROS levels (9.9 ± 2.1-fold) compared with ROS levels in fresh cells (1.0 ± 0.5-fold; Fig. 2A, B). NAC 0.4 mM reduced intracellular ROS fluorescence (Fig. 2A, white arrow) and lowered ROS levels to 1.9 ± 0.8-fold, comparable to α-TCP effects (2.0 ± 0.8-fold; Fig. 2B). These results show that NAC significantly reduced intracellular ROS levels after thawing.

3.3. NAC selectively suppresses the activation of extrinsic apoptotic signaling after thawing

Western blotting was used to examine apoptotic signaling after thawing. Freeze–thawing induced the expression of FAS, cleaved caspase-8, cleaved caspase-3, cleaved caspase-7, and cytochrome c in the vehicle group (Fig. 3A, B), indicating the activation of the extrinsic apoptotic pathway. NAC markedly reduced the expression of these proteins and showed greater suppression of apoptosis signaling than α-TCP. In contrast, intrinsic apoptosis markers—BCL-2, BAX, and cleaved caspase-9—showed limited changes after NAC treatment (Fig. S2A, B).

3.4. The phenotype of germ cells enriched for SSCs is maintained after NAC treatment

To assess whether NAC affects the germ cells enriched for SSCs phenotype, immunocytochemistry was performed using GFRα1, promyelocytic leukemia zinc finger protein (PLZF; undifferentiated spermatogonia), VASA (germ cell marker), and c-Kit (differentiated spermatogonia; Fig. 4).

Across all conditions, c-Kit expression remained negligible (Fig. S3A–B), indicating no thawing-induced differentiation. GFRα1, PLZF, and VASA were expressed at comparable levels in vehicle- and NAC-treated germ cells enriched for SSCs. These data show comparable expression of germ cells and

spermatogonial markers between the vehicle- and NAC-treated groups after thawing.

3.5. NAC enhances functional engraftment of thawed SSCs

To determine whether NAC-mediated recovery translated into functional benefits, thawed $EGFP^+$ germ cells enriched for SSCs were transplanted into busulfan-treated recipient testes and analyzed two months later (Fig. 5A). The number of SSC-derived colonies per 10^5 transplanted cells did not differ significantly between the vehicle and NAC groups (Fig. 5B, C). However, when normalized to the total number of recovered cells after culture, the overall colony-forming capacity was higher in the NAC group (889.7 ± 686.4 vs. 1903.5 ± 1616.9 colonies, $p < 0.01$; Fig. 5D). Histological analysis further confirmed the successful engraftment of NAC-treated SSCs within seminiferous tubules and their contribution to spermatogenic progression, as supported by PNA and DAPI co-localization (Fig. 5E). Collectively, NAC 0.4 mM reduced freeze-thaw-induced ROS accumulation and apoptotic signaling, maintained the phenotype of germ cells enriched for SSCs, and increased colony-forming activity after transplantation (Fig. 6).

4. Discussion

SSCs are indispensable for lifelong spermatogenesis but exhibit pronounced sensitivity to cryoinjury, often resulting in reduced viability and limited recovery following thawing. Previous efforts to improve SSC preservation have largely focused on optimizing cryoprotective formulations and freezing conditions [14, 30-34]. In contrast, the immediate post-thaw period—when oxidative stress and cellular damage are most pronounced [16, 18]—has received comparatively less attention as a therapeutic window. In this study, we demonstrated that short-term antioxidant treatment during early post-thaw recovery effectively attenuates cryo-induced cellular damage and enhances functional SSC recovery. This post-thaw-centered strategy provides a mechanistically informed and practically applicable approach that complements existing cryopreservation protocols.

To identify an effective antioxidant for this post-thaw intervention, we compared NAC, sodium selenite, and parthenolide levels during early recovery (Fig. S1). Although all three compounds have been implicated in cellular redox-related pathways [35-37], they differ markedly in their ability to restore post-thaw germ cells enriched for SSCs proliferation. Sodium selenite shows limited efficacy within a short treatment window, consistent with its reliance on prolonged exposure to GPx-mediated cytoprotection [38, 39]. Parthenolide produced a measurable improvement in post-thaw proliferation at its optimal concentration, exceeding the effect of sodium selenite, but remaining less

414 effective than NAC, in line with reports that its effective range may be constrained
415 by concentration-dependent cytotoxicity in other cell types [40]. In contrast, NAC
416 consistently produced the most robust and reproducible enhancement in post-thaw
417 recovery, providing a clear rationale for its selection for further analysis.

418 Freeze-thaw injury is associated with a rapid increase in intracellular
419 ROS [16, 41, 42]. The 12 h intervention window used in this study was selected
420 because the early post-thaw recovery phase has been reported as a period during
421 which oxidative stress and apoptotic signaling become particularly pronounced.
422 Consistent with these observations, our preliminary assessments also indicated a
423 tendency for increased apoptotic signaling within the first 12 h after thawing. To
424 investigate the mechanisms underlying NAC-mediated post-thaw recovery, we
425 examined oxidative stress and apoptosis at 12 h after freeze-thawing. NAC
426 markedly suppressed the acute ROS surge immediately after thawing, reducing
427 intracellular ROS to levels comparable to those in the α-TCP-treated group (Fig.
428 2), which was used as a positive control based on its established efficacy in SSC
429 cryopreservation [22]. This finding reinforces the idea that oxidative stress is a
430 primary early driver of cryoinjury and identifies NAC as an effective post-thaw
431 redox modulator [16, 41]. However, treatment duration may influence SSC
432 recovery, and prolonged exposure requires evaluation of its effects on SSC
433 phenotype and functional maintenance. Future studies are needed to determine
434 the optimal post-thaw intervention window.

Consistent with reduced ROS, NAC selectively attenuated extrinsic apoptotic signaling, as evidenced by the decreased activation of FAS and downstream effector caspases (Fig. 3), while intrinsic mitochondrial apoptosis markers remained largely unchanged (Fig. S2). This pattern suggests that NAC enhances post-thaw germ cells enriched for SSCs survival primarily by suppressing ROS-driven extrinsic apoptotic signaling via death receptors during the early recovery phase rather than reversing established mitochondrial dysfunction. Collectively, these findings indicate that NAC regulates ROS-dependent apoptotic signaling by modulating intracellular redox balance rather than acting as a direct ROS scavenger [43, 44].

This pattern may reflect the specific cellular stresses that arise during the early post-thaw recovery phase. Freeze-thaw injury can rapidly perturb plasma membrane integrity and induce oxidative stress during the early post-thaw recovery phase [45, 46]. Because extrinsic apoptotic signaling is initiated through membrane-associated death receptors, this pathway may be particularly sensitive to early cellular stress triggered by membrane perturbation and redox imbalance [19, 47]. In contrast, activation of the intrinsic mitochondrial pathway generally involves additional intracellular signaling events and may become more prominent during later stages of cellular recovery [48, 49]. In this context, the preferential suppression of extrinsic apoptotic signaling observed following NAC treatment may reflect modulation of early stress signals associated with freeze-thaw–induced membrane damage and oxidative imbalance during the

immediate post-thaw period. These findings suggest that apoptotic signaling following SSC cryopreservation may occur in a temporally regulated manner, with early post-thaw cellular stress preferentially activating membrane-associated apoptotic pathways before later mitochondrial involvement becomes prominent.

In comparison with α-TCP reported in our previous work, the present study further demonstrates that NAC offers several distinct advantages as a post-thaw antioxidant intervention. Unlike α-TCP, whose lipid solubility and susceptibility to oxidation may limit concentration reproducibility during short-term aqueous culture, NAC is fully water-soluble and chemically stable, allowing homogeneous distribution and precise dose control during transient post-thaw exposure. Importantly, NAC exhibits low toxicity even at relatively high concentrations and has been widely used across human and animal systems [44]. Mechanistically, α-TCP primarily functions as a membrane-associated ROS scavenger, whereas NAC acts as a redox modulator by replenishing the intracellular glutathione pool and restoring redox buffering capacity [43, 50], a distinction consistent with the observed reduction in ROS accumulation and selective attenuation of extrinsic apoptotic signaling in this study (Figs. 2, 3). Taken together, these features indicate that NAC provides practical and mechanistic advantages over α-TCP for reproducible and controllable post-thaw antioxidant intervention.

Given these advantages, it was essential to determine whether NAC-mediated cytoprotection preserves not only cell survival but also the fundamental identity of germ cells enriched for SSCs. Since improved survival alone does not necessarily reflect maintenance of stem cell function [51, 52], we next assessed whether NAC-mediated cytoprotection affected germ cells enriched for SSCs identity or differentiation status (Fig. 4). Immunophenotypic analyses demonstrated that key undifferentiated spermatogonia markers (GFRα1 and PLZF) and the germ cell marker (VASA) remained stably expressed following NAC treatment, whereas the differentiation marker (c-Kit) remained undetectable across all groups. These results indicate that transient antioxidant exposure during early recovery enhances germ cells enriched for SSCs survival without inducing phenotypic drift or aberrant differentiation. Importantly, this finding establishes that NAC-mediated post-thaw recovery reflects the functional preservation of germ cells enriched for SSCs rather than survival at the expense of stemness, underscoring its suitability for applications that require strict maintenance of germline integrity.

Building on this phenotypic stability, the functional relevance of NAC-mediated recovery was evaluated in vivo (Fig. 5). Although NAC treatment did not alter the intrinsic colony-forming frequency per transplanted cell, it significantly increased the total pool of transplantable, functional SSCs by improving the efficiency of post-thaw recovery. This distinction is critical, as it indicates that NAC acts primarily by expanding the number of viable, functionally

competent SSCs available for engraftment, rather than by artificially enhancing the self-renewal capacity. Successful engraftment and the progression into spermatogenesis further support the idea that NAC-treated SSCs retain full regenerative competence within the testicular niche [53]. Collectively, these findings indicate that NAC-mediated cytoprotection during early post-thaw recovery translates into meaningful gains in the number of functionally competent SSCs available for transplantation. Taken together, our results support NAC as a practical and effective post-thaw adjunct for improving the recovery and functional availability of cryopreserved SSCs, with clear relevance for fertility preservation and germline conservation.

While the present study focused on antioxidant intervention during the early post-thaw recovery phase, oxidative and apoptotic damage may also arise during the freezing process itself [45]. Antioxidant supplementation during freezing may therefore represent an additional strategy to mitigate cryoinjury, although its effects are likely to depend on the specific cryopreservation conditions. Accordingly, the present study did not evaluate NAC as a freezing additive but instead examined whether transient NAC treatment after thawing could improve germ cells enriched for SSCs recovery under an established trehalose-based freezing condition. Future studies will be needed to determine whether NAC supplementation during freezing, alone or in combination with post-thaw treatment, provides additional benefit for SSC cryopreservation.

5. Conclusions

The results of this study demonstrate that short-term antioxidant intervention during the early post-thaw period represents an effective and conceptually distinct strategy for improving germ cells enriched for SSCs recovery after cryopreservation. By targeting the acute oxidative and apoptotic stress that arises immediately after thawing, NAC preserves germ cells enriched for SSCs viability while maintaining phenotypic identity and in vivo regenerative competence. Importantly, this approach enhances the absolute yield of functional SSCs without altering their intrinsic self-renewal properties, thereby overcoming the major limitations of conventional cryopreservation protocols that primarily focus on freezing conditions. These findings establish post-thaw redox modulation as a critical and previously underappreciated determinant of SSC recovery and provide a practical framework for integrating antioxidant-based recovery steps into existing fertility preservation and germline conservation strategies. Within this framework, NAC offers practical advantages over α-TCP for post-thaw antioxidant intervention through its aqueous stability, low toxicity, and glutathione-mediated redox modulation, thereby enabling reproducible recovery of functional SSCs.

This post-thaw-centered approach has direct implications for animal reproduction, as SSC cryopreservation is increasingly being recognized as a foundational technology for assisted reproduction, genetic resource conservation, and breeding strategies in livestock and experimental animal models. By

improving the efficiency of functional SSC recovery without compromising the stem cell identity, the present findings support the broad application of post-thaw redox modulation as a versatile and translatable platform for reproductive biotechnology across species.

CRediT Authorship Contribution Statement

Eun-Ji Paeng: Conceptualization, Formal analysis, Methodology, Visualization, Writing – original draft. **Sang-Eun Jung**: Data curation, Validation, Visualization, Writing – review & editing. **Hyo Jin Gu**: Investigation, Formal analysis. **Sung-Hwan Moon**: Resources, Writing – review & editing. **Seung Hee Shin**: Methodology, Validation, Writing – review & editing. **Buom-Yong Ryu**: Conceptualization, Funding acquisition, Project administration, Resources, Supervision, Validation, Writing – review & editing.

Declaration of Competing Interests

The authors declare no competing interests.

Acknowledgement

We thank J. Kim at the BT Research Facility Center, Chung-Ang University for technical assistance. Figures were created with BioRender.com.

Funding

This study was supported by the National Research Foundation of Korea (NRF) funded by the Ministry of Science and ICT (RS-2024-00347342).

References

1. Goodyear S, Brinster R. Spermatogonial Stem Cell Transplantation to the Testis. Cold Spring Harb Protoc. 2017;2017(4):pdb.prot094235. https://doi.org/10.1101/pdb.prot094235

2. Li L, Xie T. Stem cell niche: structure and function. Annu Rev Cell Dev Biol. 2005;21:605–31. https://doi.org/10.1146/annurev.cellbio.21.012704.131525

3. Patel H, Bhartiya D. Testicular Stem Cells Express Follicle-Stimulating Hormone Receptors and Are Directly Modulated by FSH. Reprod Sci. 2016;23(11):1493–508. https://doi.org/10.1177/1933719116643593

4. Dym M, Fawcett DW. Further observations on the numbers of spermatogonia, spermatocytes, and spermatids connected by intercellular bridges in the mammalian testis. Biol Reprod. 1971;4(2):195–215. https://doi.org/10.1093/biolreprod/4.2.195

5. He S, Nakada D, Morrison SJ. Mechanisms of stem cell self-renewal. Annu Rev Cell Dev Biol. 2009;25:377–406. https://doi.org/10.1146/annurev.cellbio.042308.113248

6. Oatley JM, Brinster RL. Spermatogonial stem cells. Methods Enzymol. 2006;419:259–82. https://doi.org/10.1016/s0076-6879(06)19011-4

7. Mann U, Shiff B, Patel P. Reasons for worldwide decline in male fertility. Curr Opin Urol. 2020;30(3):296–301. https://doi.org/10.1097/mou.0000000000000745

8. Sadri-Ardekani H, Atala A. Testicular tissue cryopreservation and spermatogonial stem cell transplantation to restore fertility: from bench to bedside. Stem Cell Res Ther. 2014;5(3):68. https://doi.org/10.1186/scrt457

9. Goossens E, Van Saen D, Tournaye H. Spermatogonial stem cell preservation and transplantation: from research to clinic. Hum Reprod. 2013;28(4):897–907. https://doi.org/10.1093/humrep/det039

10. Picton HM, Wyns C, Anderson RA, Goossens E, Jahnukainen K, Kliesch S, et al. A European perspective on testicular tissue cryopreservation for fertility preservation in prepubertal and adolescent boys. Hum Reprod. 2015;30(11):2463–75. https://doi.org/10.1093/humrep/dev190

11. Bissoyi A, Nayak B, Pramanik K, Sarangi SK. Targeting cryopreservation-induced cell death: a review. Biopreserv Biobank. 2014;12(1):23–34. https://doi.org/10.1089/bio.2013.0032

12. Du L, Chen W, Cheng Z, Wu S, He J, Han L, et al. Novel Gene Regulation in Normal and Abnormal Spermatogenesis. Cells. 2021;10(3). https://doi.org/10.3390/cells10030666

13. Avarbock MR, Brinster CJ, Brinster RL. Reconstitution of spermatogenesis from frozen spermatogonial stem cells. Nat Med. 1996;2(6):693–6. https://doi.org/10.1038/nm0696-693

14. Jung SE, Kim M, Ahn JS, Kim YH, Kim BJ, Yun MH, et al. Effect of Equilibration Time and Temperature on Murine Spermatogonial Stem Cell Cryopreservation. Biopreserv Biobank. 2020;18(3):213–21. https://doi.org/10.1089/bio.2019.0116

15. Yang F, Zhao J, Li Y, Niu C, Zheng Y. Cryopreservation of spermatogonial stem cells: an overview of cryoprotectants. Reprod Biomed Online. 2025;51(4):105023. https://doi.org/10.1016/j.rbmo.2025.105023

16. Len JS, Koh WSD, Tan SX. The roles of reactive oxygen species and antioxidants in cryopreservation. Biosci Rep. 2019;39(8). https://doi.org/10.1042/bsr20191601

17. Brentnall M, Rodriguez-Menocal L, De Guevara RL, Cepero E, Boise LH. Caspase-9, caspase-3 and caspase-7 have distinct roles during intrinsic apoptosis. BMC Cell Biol. 2013;14:32. https://doi.org/10.1186/1471-2121-14-32

18. Coundouris JA, Grant MH, Engeset J, Petrie JC, Hawksworth GM. Cryopreservation of human adult hepatocytes for use in drug metabolism and toxicity studies. Xenobiotica. 1993;23(12):1399–409. https://doi.org/10.3109/00498259309059449

19. Heng BC, Clement MV, Cao T. Caspase inhibitor Z-VAD-FMK enhances the freeze-thaw survival rate of human embryonic stem cells. Biosci Rep. 2007;27(4-5):257–64. https://doi.org/10.1007/s10540-007-9051-2

20. Sasnoor LM, Kale VP, Limaye LS. Prevention of apoptosis as a possible mechanism behind improved cryoprotection of hematopoietic cells by catalase and trehalose. Transplantation. 2005;80(9):1251–60. https://doi.org/10.1097/01.tp.0000169028.01327.90

21. Ha SJ, Kim BG, Lee YA, Kim YH, Kim BJ, Jung SE, et al. Effect of Antioxidants and Apoptosis Inhibitors on Cryopreservation of Murine Germ Cells Enriched for Spermatogonial Stem Cells. PLoS One. 2016;11(8):e0161372. https://doi.org/10.1371/journal.pone.0161372

22. Jung SE, Oh HJ, Ahn JS, Kim YH, Kim BJ, Ryu BY. Antioxidant or Apoptosis Inhibitor Supplementation in Culture Media Improves Post-Thaw Recovery of Murine Spermatogonial Stem Cells. Antioxidants (Basel). 2021;10(5). https://doi.org/10.3390/antiox10050754

633 23. Kubota H, Avarbock MR, Brinster RL. Growth factors essential for self-renewal
634 and expansion of mouse spermatogonial stem cells. Proc Natl Acad Sci U S A.
635 2004;101(47):16489–94. https://doi.org/10.1073/pnas.0407063101
636 24. Lee YA, Kim YH, Kim BJ, Kim BG, Kim KJ, Auh JH, et al. Cryopreservation in
637 trehalose preserves functional capacity of murine spermatogonial stem cells. PLoS One.
638 2013;8(1):e54889. https://doi.org/10.1371/journal.pone.0054889
639 25. Shin BJ, Kim BJ, Paeng EJ, Rifkin JT, Moon SH, Shin SH, et al. N-Acetyl-L-
640 cysteine attenuates titanium dioxide nanoparticle (TiO(2) NP)-induced autophagy in
641 male germ cells. Environ Toxicol Pharmacol. 2024;108:104466.
642 https://doi.org/10.1016/j.etap.2024.104466
643 26. Brinster RL. Germline stem cell transplantation and transgenesis. Science
644 (New York, NY). 2002;296(5576):2174–6. https://doi.org/10.1126/science.1071607
645 27. Brinster RL, Avarbock MR. Germline transmission of donor haplotype
646 following spermatogonial transplantation. Proc Natl Acad Sci U S A.
647 1994;91(24):11303–7. https://doi.org/10.1073/pnas.91.24.11303
648 28. Ogawa T, Arechaga JM, Avarbock MR, Brinster RL. Transplantation of testis
649 germinal cells into mouse seminiferous tubules. The International journal of
650 developmental biology. 1997;41(1):111–22.
651 29. Kim SH, Shin SH, Kim SM, Jung SE, Shin BJ, Ahn JS, et al. Bisphenol Analogs
652 Downregulate the Self-Renewal Potential of Spermatogonial Stem Cells. World J Mens
653 Health. 2025;43(1):154–65. https://doi.org/10.5534/wjmh.230166
654 30. Jung SE, Ahn JS, Kim YH, Kim BJ, Won JH, Ryu BY. Effective cryopreservation
655 protocol for preservation of male primate (Macaca fascicularis) prepubertal fertility.
656 Reprod Biomed Online. 2020;41(6):1070–83.
657 https://doi.org/10.1016/j.rbmo.2020.07.016
658 31. Jung SE, Ahn JS, Kim YH, Kim SM, Um TG, Kim BJ, et al. Inhibition of Caspase-
659 8 Activity Improves Freezing Efficiency of Male Germline Stem Cells in Mice. Biopreserv
660 Biobank. 2021;19(6):493–502. https://doi.org/10.1089/bio.2021.0017
661 32. Jung SE, Ahn JS, Kim YH, Oh HJ, Kim BJ, Kim SU, et al. Autophagy modulation
662 alleviates cryoinjury in murine spermatogonial stem cell cryopreservation. Andrology.
663 2022;10(2):340–53. https://doi.org/10.1111/andr.13105
664 33. Jung SE, Ahn JS, Kim YH, Oh HJ, Kim BJ, Ryu BY. Necrostatin-1 improves the
665 cryopreservation efficiency of murine spermatogonial stem cells via suppression of
666 necroptosis and apoptosis. Theriogenology. 2020;158:445–53.

https://doi.org/10.1016/j.theriogenology.2020.10.004
34. Jung SE, Jin JH, Ahn JS, Kim YH, Yun MH, Kim SH, et al. Effect of serum replacement on murine spermatogonial stem cell cryopreservation. Theriogenology. 2021;159:165–75. https://doi.org/10.1016/j.theriogenology.2020.10.037
35. Rushworth GF, Megson IL. Existing and potential therapeutic uses for N-acetylcysteine: the need for conversion to intracellular glutathione for antioxidant benefits. Pharmacol Ther. 2014;141(2):150–9. https://doi.org/10.1016/j.pharmthera.2013.09.006
36. Kurdi M, Bowers MC, Dado J, Booz GW. Parthenolide induces a distinct pattern of oxidative stress in cardiac myocytes. Free Radic Biol Med. 2007;42(4):474–81. https://doi.org/10.1016/j.freeradbiomed.2006.11.012
37. Brigelius-Flohé R, Maiorino M. Glutathione peroxidases. Biochim Biophys Acta. 2013;1830(5):3289–303. https://doi.org/10.1016/j.bbagen.2012.11.020
38. Abo El-Magd NF, Barbosa PO, Nick J, Covalero V, Grignetti G, Bermano G. Selenium, as selenite, prevents adipogenesis by modulating selenoproteins gene expression and oxidative stress-related genes. Nutrition. 2022;93:111424. https://doi.org/10.1016/j.nut.2021.111424
39. Lee JG, Jang JY, Baik SM. Selenium as an Antioxidant: Roles and Clinical Applications in Critically Ill and Trauma Patients: A Narrative Review. Antioxidants (Basel). 2025;14(3). https://doi.org/10.3390/antiox14030294
40. Tsai TY, Chan P, Gong CL, Wong KL, Su TH, Shen PC, et al. Parthenolide-Induced Cytotoxicity in H9c2 Cardiomyoblasts Involves Oxidative Stress. Acta Cardiol Sin. 2015;31(1):33–41. https://doi.org/10.6515/acs20140422b
41. Nazeri T, Hedayatpour A, Kazemzadeh S, Safari M, Safi S, Khanehzad M. Antioxidant Effect of Melatonin on Proliferation, Apoptosis, and Oxidative Stress Variables in Frozen-Thawed Neonatal Mice Spermatogonial Stem Cells. Biopreserv Biobank. 2022;20(4):374–83. https://doi.org/10.1089/bio.2021.0128
42. Zhang D, Ren L, Chen GQ, Zhang J, Reed BM, Shen XH. ROS-induced oxidative stress and apoptosis-like event directly affect the cell viability of cryopreserved embryogenic callus in Agapanthus praecox. Plant Cell Rep. 2015;34(9):1499–513. https://doi.org/10.1007/s00299-015-1802-0
43. Aldini G, Altomare A, Baron G, Vistoli G, Carini M, Borsani L, et al. N-Acetylcysteine as an antioxidant and disulphide breaking agent: the reasons why. Free Radic Res. 2018;52(7):751–62. https://doi.org/10.1080/10715762.2018.1468564

44. Samuni Y, Goldstein S, Dean OM, Berk M. The chemistry and biological activities of N-acetylcysteine. Biochim Biophys Acta. 2013;1830(8):4117–29. https://doi.org/10.1016/j.bbagen.2013.04.016
45. Murray KA, Gibson MI. Chemical approaches to cryopreservation. Nat Rev Chem. 2022;6(8):579–93. https://doi.org/10.1038/s41570-022-00407-4
46. Gao D, Critser JK. Mechanisms of cryoinjury in living cells. Ilar j. 2000;41(4):187–96. https://doi.org/10.1093/ilar.41.4.187
47. Elmore S. Apoptosis: a review of programmed cell death. Toxicol Pathol. 2007;35(4):495–516. https://doi.org/10.1080/01926230701320337
48. Galluzzi L, Vitale I, Aaronson SA, Abrams JM, Adam D, Agostinis P, et al. Molecular mechanisms of cell death: recommendations of the Nomenclature Committee on Cell Death 2018. Cell Death Differ. 2018;25(3):486–541. https://doi.org/10.1038/s41418-017-0012-4
49. Mustafa M, Ahmad R, Tantry IQ, Ahmad W, Siddiqui S, Alam M, et al. Apoptosis: A Comprehensive Overview of Signaling Pathways, Morphological Changes, and Physiological Significance and Therapeutic Implications. Cells. 2024;13(22). https://doi.org/10.3390/cells13221838
50. Traber MG, Atkinson J. Vitamin E, antioxidant and nothing more. Free Radic Biol Med. 2007;43(1):4–15. https://doi.org/10.1016/j.freeradbiomed.2007.03.024
51. Morrison SJ, Kimble J. Asymmetric and symmetric stem-cell divisions in development and cancer. Nature. 2006;441(7097):1068–74. https://doi.org/10.1038/nature04956
52. Clevers H, Watt FM. Defining Adult Stem Cells by Function, not by Phenotype. Annu Rev Biochem. 2018;87:1015–27. https://doi.org/10.1146/annurev-biochem-062917-012341
53. Brinster RL, Zimmermann JW. Spermatogenesis following male germ-cell transplantation. Proc Natl Acad Sci U S A. 1994;91(24):11298–302. https://doi.org/10.1073/pnas.91.24.11298

730 **Figure legends**

731

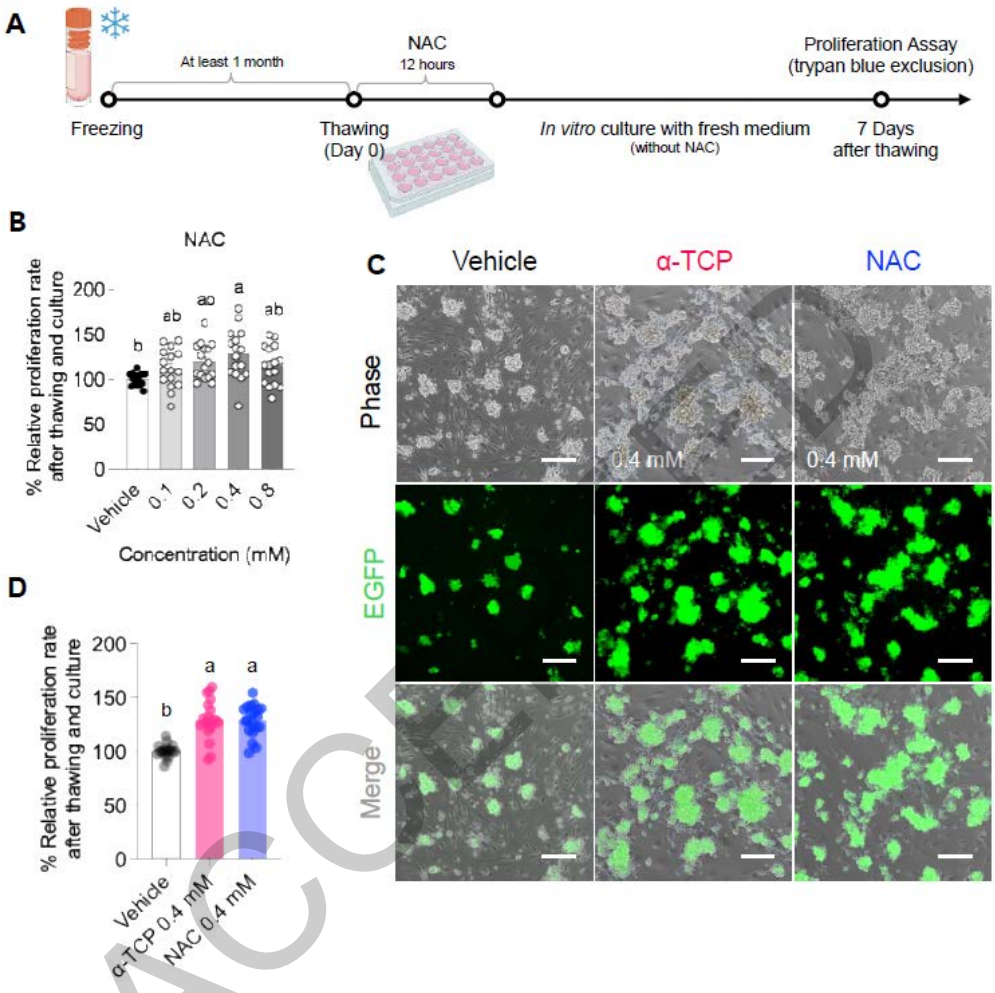

732
733

734 **Fig. 1.** Evaluation of post-thaw proliferation of germ cells enriched for SSCs
735 following NAC treatment. (A) Experimental scheme illustrating the
736 cryopreservation, thawing, and subsequent culture procedures. Germ cells
737 enriched for SSCs were treated with various concentrations of NAC for 12 h after
738 thawing and cultured for 7 days. (B) Proliferation rates determined using trypan

739 blue exclusion assays after 7 days of in vitro culture (n = 16). (C) Representative
740 bright-field and fluorescence images of $EGFP^+$ germ cells enriched for SSCs
741 colonies treated with 0.4 mM α-TCP (positive control) or 0.4 mM NAC. α-TCP
742 served as a positive control based on our previous study. (D) Quantitative
743 comparison of proliferation rates between the α-TCP (0.4 mM) and NAC (0.4 mM)
744 treatments (n = 20). Data represent the mean ± SEM of independent experiments,
745 and each dot represents an individual value. Statistical significance was
746 determined using one-way ANOVA followed by Tukey's post-hoc test. Different
747 letters above the bars indicate statistically significant differences ($p < 0.05$). Scale
748 bars = 200 μm.
749

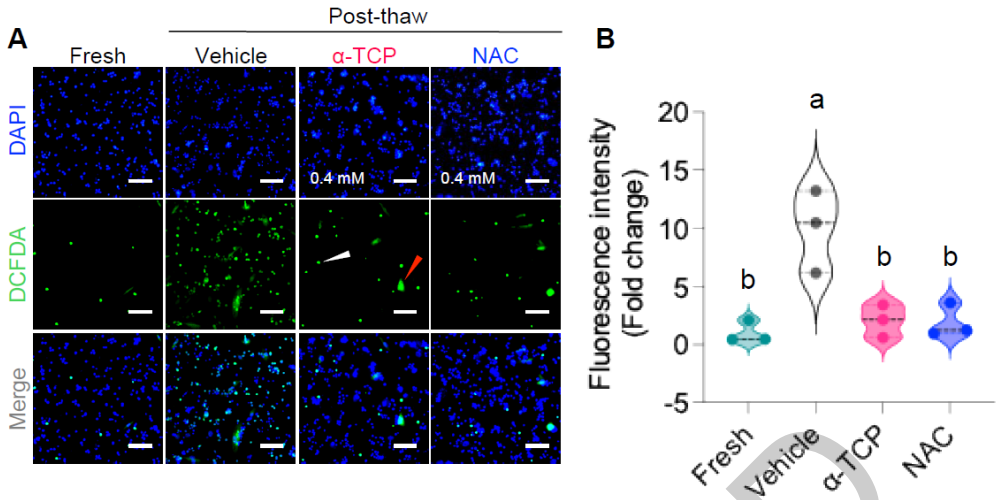

750

751

752 **Fig. 2.** Immediate ROS generation following thawing of germ cells enriched for
753 SSCs and its attenuation by antioxidant treatment. (A) Representative
754 fluorescence images showing intracellular ROS levels detected by DCFDA (green)
755 and nuclei stained with DAPI (blue) after a 12 h incubation with or without
756 antioxidants. The fresh group indicates the non-frozen control, whereas α-TCP,
757 0.4 mM, and NAC, 0.4 mM, were used as antioxidant treatments. White
758 arrowheads indicate germ cells enriched for SSCs, and red arrowheads indicate
759 STO feeder cells. Scale bar = 100 μm. (B) Quantitative analysis of ROS
760 fluorescence intensity presented as violin plots normalized to cell number. Each
761 dot represents an individual value. Data represent the mean ± SEM of three
762 independent experiments, and each dot represents an individual value. Statistical
763 significance was determined using one-way ANOVA followed by Tukey's post-

hoc test. Different letters above the bars indicate statistically significant differences ($p < 0.05$).

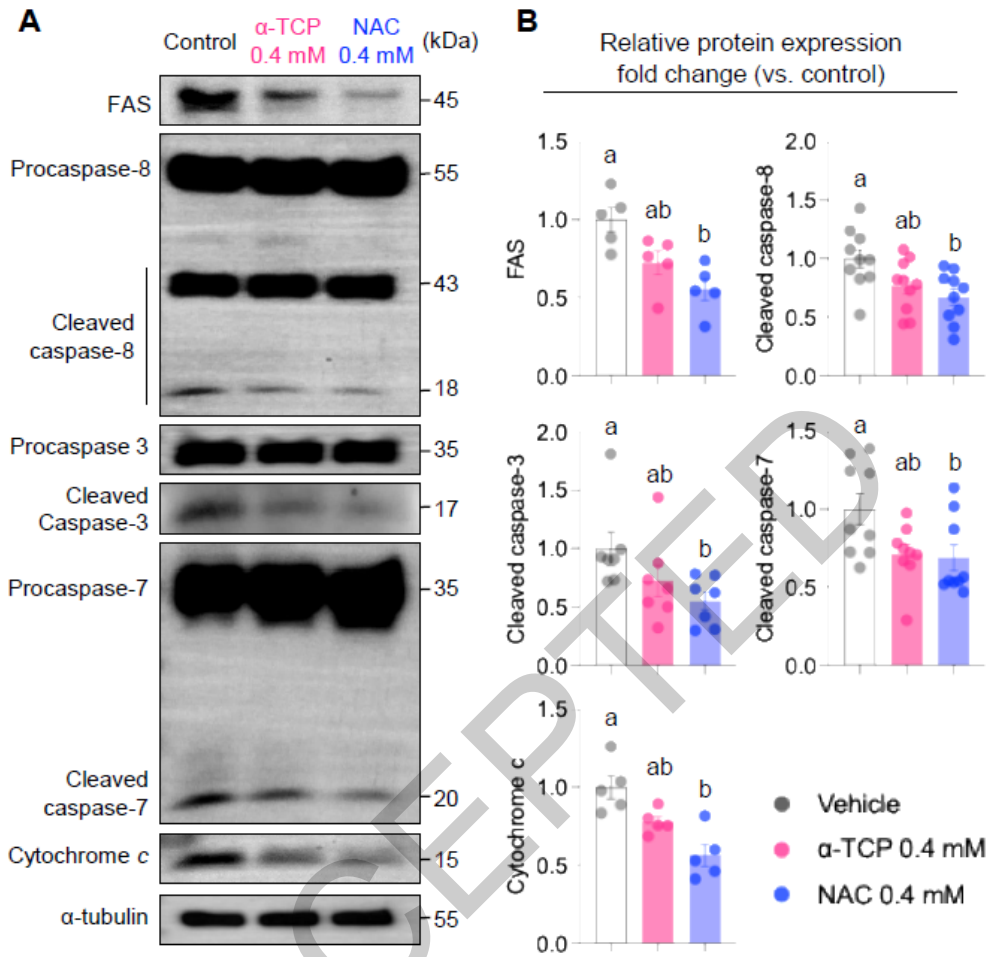

767

768 **Fig. 3.** Effects of NAC on apoptosis-related protein expression in germ cells
769 enriched for SSCs following cryopreservation. (A) Representative western blot
770 images showing the expression of apoptosis-associated proteins, including FAS,
771 cleaved caspase-8, -3, -7, and cytochrome c, in groups treated with vehicle, α-
772 TCP (0.4 mM, positive control), or NAC (0.4 mM). α-Tubulin serves as the
773 loading control. (B) Quantitative analysis of relative protein levels normalized to
774 α-tubulin and expressed as fold change versus the vehicle group. Data represent

775 the mean ± SEM of independent experiments (FAS, $n = 5$; cleaved caspase-8, $n =$
776 10; cleaved caspase-3, $n = 7$; cleaved caspase-7, $n = 9$; cytochrome c, $n = 5$), and
777 each dot represents an individual value. Statistical significance was determined
778 using one-way ANOVA followed by Tukey's post-hoc test. Different letters above
779 the bars indicate statistically significant differences ($p < 0.05$).
780

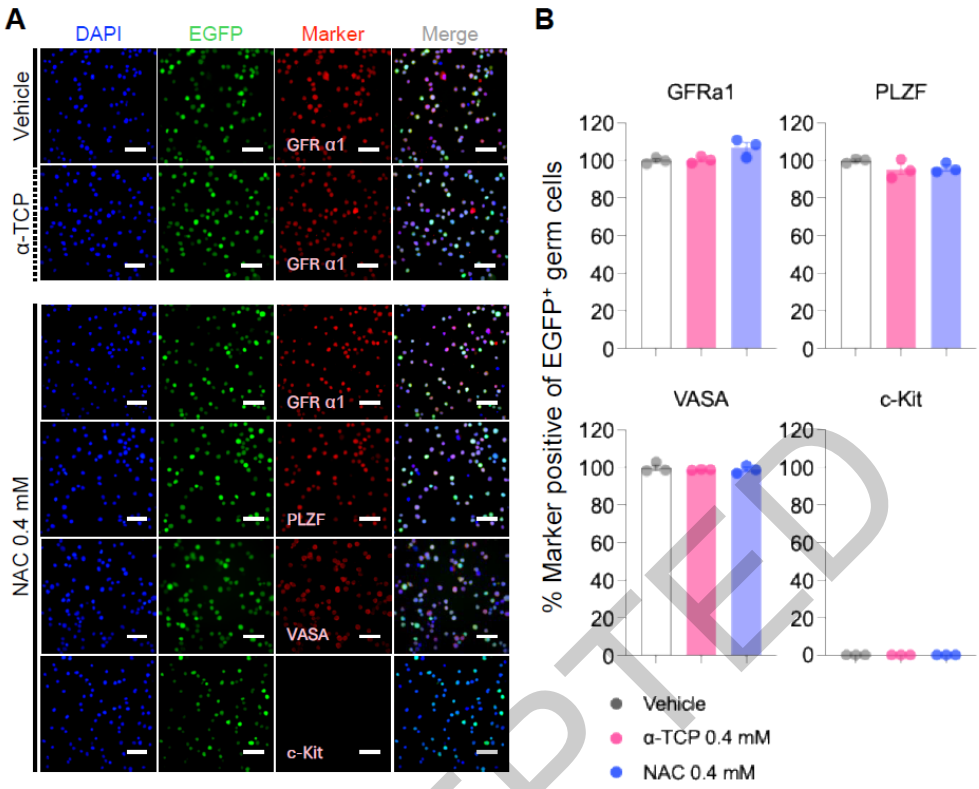

781

782 **Fig. 4.** Antioxidant treatment during post-thaw recovery preserves germ cells
783 enriched for SSCs characteristics. (A) Representative immunofluorescence
784 images of germ cells enriched for SSCs following antioxidant treatment after
785 thawing. Undifferentiated spermatogonia are identified by GFRα1 (red) and
786 PLZF (red) expression, whereas germ cells and differentiated spermatogonia
787 express VASA (red) and c-Kit (red), respectively. Nuclei are stained with DAPI
788 (blue), and EGFP (green) indicates $EGFP^+$ germ cells enriched for SSCs. Scale
789 bars = 50 μm. (B) Quantitative analysis of $EGFP^+$ germ cells enriched for SSCs
790 expressed as a percentage of DAPI-stained cells. Each dot represents an individual
791 value. Data represent the mean ± SEM of three independent experiments, and each

792 dot represents an individual value. Statistical significance was determined using
793 one-way ANOVA followed by Tukey's post-hoc test. Different letters above the
794 bars indicate statistically significant differences ($p < 0.05$).
795

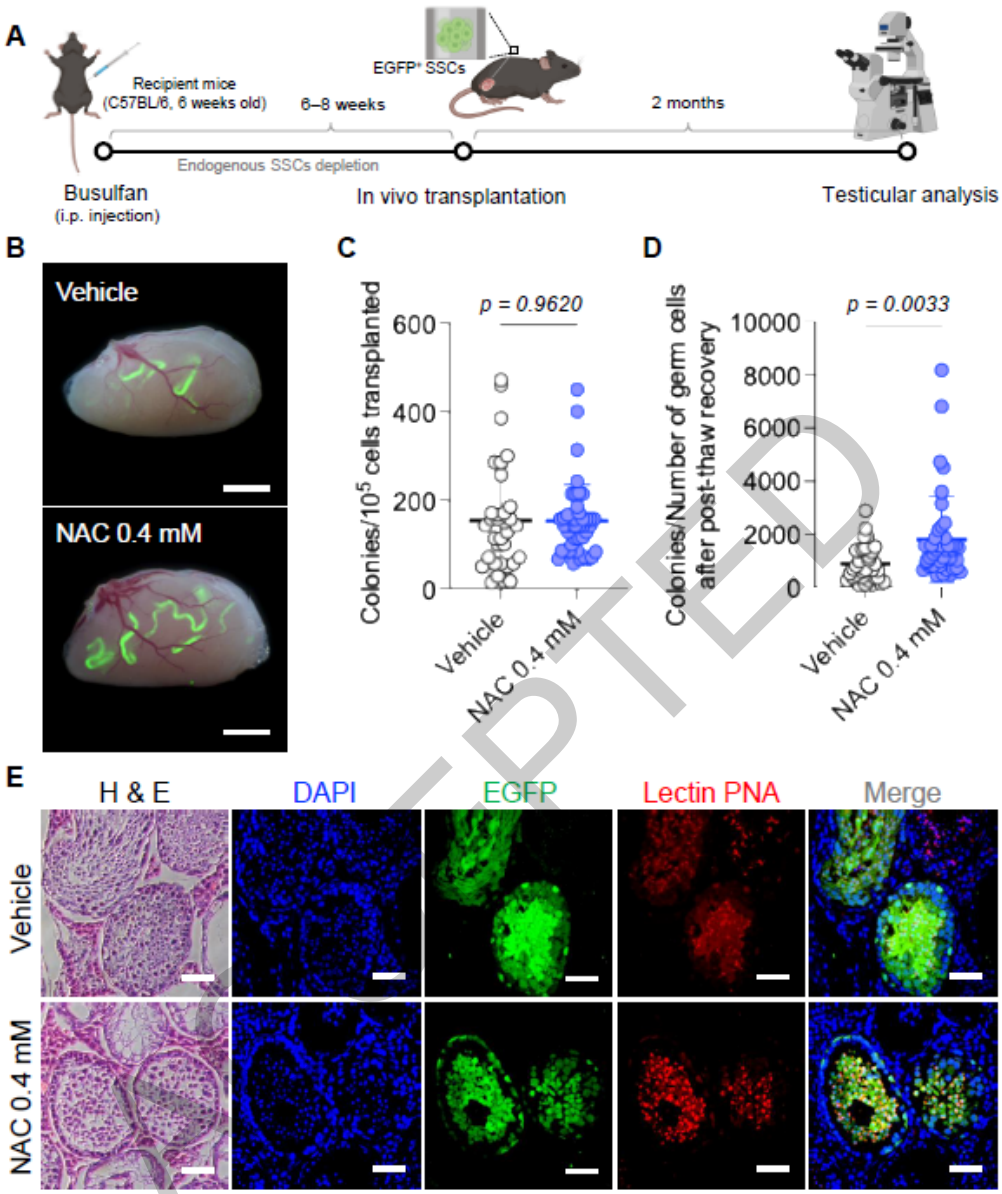

796

797 **Fig. 5.** Functional restoration of SSC activity following cryopreservation and

798 NAC treatment. (A) Schematic overview of the experimental timeline for germ

799 cells enriched for SSCs transplantation into busulfan-treated recipient mice. (B)

800 Representative dark-field fluorescence images of recipient testes merged with

bright-field views, showing donor-derived $EGFP^+$ colonies after transplantation of vehicle- or 0.4 mM NAC-treated SSCs. Scale bars = 2 mm. (C, D) Quantitative assessment of SSC activity based on colony formation. The number of $EGFP^+$ colonies was evaluated as (C) colonies formed per 10^5 transplanted germ cells enriched for SSCs and (D) colonies formed relative to the total number of cultured cells after cryopreservation followed by 0.4 mM NAC treatment 12 h after thawing. Each dot represents an individual testis. Data are presented as the mean ± SEM, and each dot represents an individual value. The vehicle group comprises 34 testes from 17 mice, and the NAC 0.4 mM group consists of 42 testes from 21 mice. Statistical significance was determined using the unpaired two-tailed Student's *t*-test. (E) Histological and immunofluorescence analyses of recipient testes 2 months after transplantation. Paraffin-embedded sections were stained with hematoxylin and eosin (H&E) and co-stained with DAPI (blue), PNA lectin (red), and anti-GFP antibody (green) to confirm donor-derived SSC colonization within the seminiferous tubules. Scale bars = 50 μm.

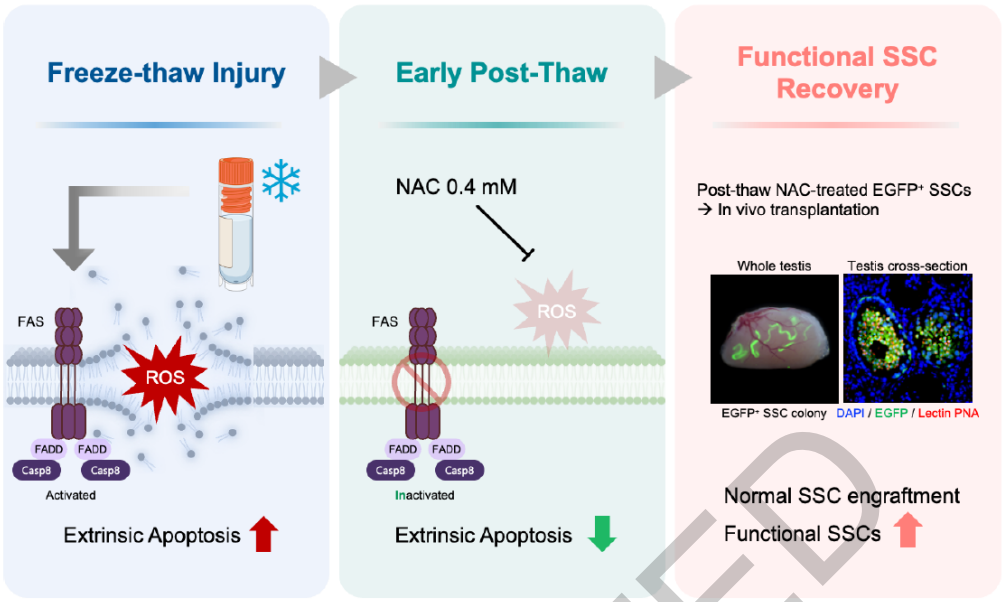

817

818 **Fig. 6.** Summary illustrating the role of early post-thaw NAC treatment in
819 improving functional recovery of SSCs after cryopreservation. Freeze–thaw
820 injury induces excessive ROS generation, leading to activation of FAS-mediated
821 extrinsic apoptotic signaling through FADD and caspase-8. NAC treatment (0.4
822 mM) during the early post-thaw period suppresses ROS accumulation and
823 attenuates extrinsic apoptosis without altering basal cellular identity. As a result,
824 post-thaw NAC-treated EGFP^{+} SSCs exhibit preserved engraftment capacity
825 following in vivo transplantation, as evidenced by normal SSC colony formation
826 in whole testis and cross-sectional analyses. This strategy enhances functional
827 SSC recovery by targeting acute post-thaw oxidative stress.